Kinematic Motion Modelling from Differential Inductive Oscillation Sensing for a Servomechanism and Electromechanical Devices and Applications

Abdulwahab Deji[1], Sheroz Khan[2], Musse Mohamoud Ahmad[3]

[1]Department of Electrical Computer Information and Telecommunication Engineering, Waidsum University Malaysia.
[2]Department of Electrical Engineering Onaizah College Saudi Arabia.
[3]Department of Electrical and Computer Engineering University of Malaysia Sarawak.

Abstract:

This paper presents mathematical modeling approach of an inductive sensor producing oscillating output of a given frequency representing displacement of a core moving in and out of a coil of known geometrical dimensions. The technique is hence used in characterizing the speed, acceleration and frequency of the proposed differential inductive transducer. This model uses a double coil arrangement with a freely movable iron core. This is made to oscillate freely thereby producing the proposed output for characterization of oscillating parameters. The application of this work finds utility in generating small amplitude signals from tiny force winds for the purpose of acquiring impulsive electrical signal from sources such as machine vibrations. Using an inductive coil sensing technique in a differential manner, physical parameters of speed, acceleration and displacement are translated into a signal with proportionate output frequency change. The results shown can be used for characterizing the materials and hence sensor with high sensitivity, linearity and responsiveness in harsh environmental condition is obtained.

Keyword: Speed, acceleration, speed-to-frequency converter, acceleration-to-frequency converter, variable inductance, magnetization, pressure sensor, displacement, relative permeability.

1. INTRODUCTION

Real time precise measurement needs circuits and instrumentation electronic for playing a significant role in designs and automation needed these days in sensing and control of smart instrumentation. The hard to reach locations with employed target devices, and their characterization, detection, and monitoring are better handled by deferentially coupled oscillatory system. These kind of oscillatory measurement circuits are important for the determination of core speed and acceleration in a magnetic coil topology coupled deferentially in an oscillatory manner. This produces a two ways movement, that is, the inward and outward within a coil with vertical orientation. Magnetic iron core possesses a variety of attractive properties, such as high electrical and thermal conductivity, high density, and serviceability; through extrusion, it is possible to create complex forms that are difficult to be achieved in any other way. Coil is the largest production facility for continuous geomagnetic topology of a see-saw oscillation orientation

strip. The results of this work also, find utility in production line equipment, loading and unloading systems [1].

Pressure sensors are broadly categorized into three varieties, namely; piezo-resistive, capacitive, Linear Variable Displacement Transducers (LVDT). Piezo-resistive sensors have the advantage of good linearity and acceptable sensitivity, but put at a disadvantage from the fact that it possesses the problem of inaccuracy due to issues from large temperature hysteresis which causes in some applications inaccuracies of unacceptable level [2]-[3]. Capacitive pressure sensors exhibit features of higher sensitivity and lower temperature hysteresis, but they are suffer from nonlinear issues more than other categories [4]-[5] even in low temperature range applications. Conventional LVDT-based pressure sensors possess good linearity, highest sensitivity and lowest temperature hysteresis, but such devices have a demerit of bulky physical structures [6]. New pressure sensor is characterized with excellent linearity, high sensitivity and a low temperature hysteresis.

This paper introduces a novel type of force sensing using concepts reported in recently reported works [2] that is characterized by: a) miniature size most suited for being used in devices buried or in inaccessible locations; b) excellent linearity over an arbitrary chosen force, speed, acceleration range; c) substantially high sensitivity; d) substantially low temperature hysteresis; e) Low power consumption; f) excellent responsiveness, g) good level of immunity to interference from neighboring environment. Each segment of this work has been characterized into different sections. Section I gives the introduction and review of contemporary work, section II describes the method adopted for this work. Section III describes the theory, derivation and force sensor design. The results are shown in section IV. Error analysis is given in section V; while conclusion is presented in section VI.

2. METHOD

The method used in this force sensitive transducer arrangement is as shown in Figure 1. This model uses double coil arrangement with iron core moving in and out in a seesaw style. This phenomenon is the result of simple movement of the core position bringing about changes in the inductance of the coils and ultimately in the frequency, duty cycle, current, voltage, force and pressure-temperature hysteresis. The idea is shown to be of applications in devices used for harvesting of energy including other applications such as in liquid level characterization. The core is made of materials of known relative permeability. The proposed sensor offers a change in inductance of 42.9mH over a pressure range of 0.3kPa to 15.3kPa while moving over a displacement of from 0 – 0.02m. Its sensitivity is therefore 2.80mH/kPa which is substantially higher than previously reported work and also when compared to results by recently reported contemporary research works. As shown in Figure 1, a coil of 6mm length and a diameter of 8mm is used. A small cylindrical iron core of a height of 6mm and a diameter of 4mm is positioned inside the coil, surrounded by a smooth insulation material. The arrangement is such that the pressure and force acts on the iron core in the upwards and downwards direction. This provides the seesaw oscillation with the upward and downward motion of the core as shown in Figure 1. In addition, a horizontal bar is positioned on top and connected to the core in both directions in order to contain the iron core as it gets displaced. The displacement of the core is proportionate to the force applied and ultimately the pressure. This creates oscillation as both cores are connected to the ends of convulsion bar. The sensor's performance parameters are as shown listed in Table 1, added on information to what is reported in [2].

Table 1: Sensor's performance indices

Types	Sensitivity	Linearity	Pre. Hyst	Tempt. Hyst	Responsiveness
Piezor.p.s	25mV/kPa	Linear	±1% FSO	±2% FSO	Quick
Cap. Pre. Sensor	0.2nF/kPa	Nonlinear	±0.1% FSO	±0.5% FSO	Slow
LVDT	400mV/kPa	Linear	±0.5% FSO	±0.1% FSO	Slow
Mass Sensor	3.56mH/kPa	Linear	±0.05% FSO	±0.1% FSO	Average
Wind Sensor	2.93KHz/kPa	Highly Linear	±0.02% FSO	±0.01% FSO	Quick
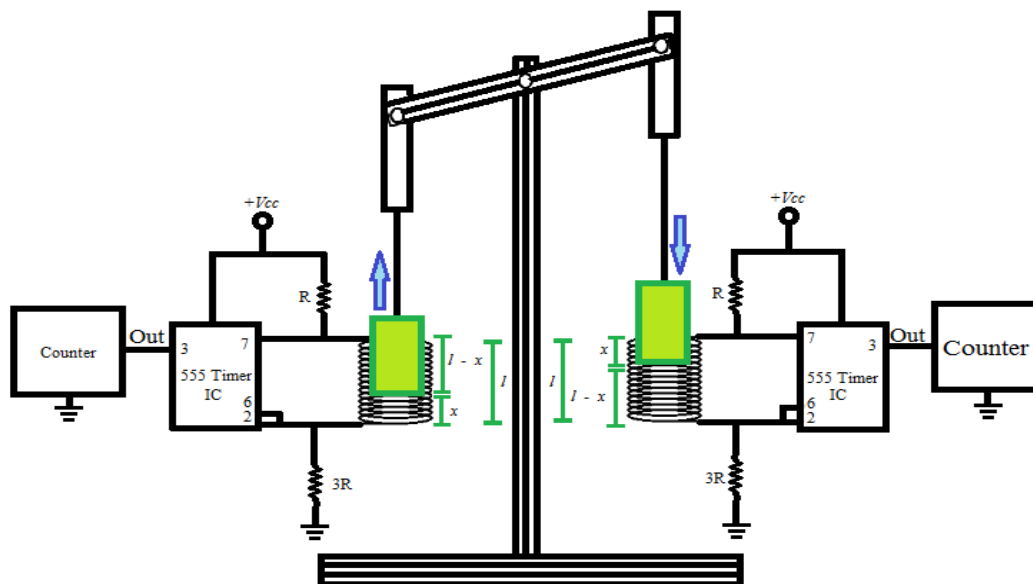
Figure 1: A conceptual design of convulsion bar resting on a pivot point moving in a sea saw manner over two magnetic coils:

3. THEORY OF OPERATION AND DERIVATION

From the convulsion bar shown in Figure 1, a little force as a result of pressure over an area is applied to the right side of the seesaw bar, which causes downward displacement of the magnetic core within the coils resulting to an inductive change. This change is proportional to the physical parameter of interest such as the acceleration, speed, force, pressure and frequency, duty cycle. The core on the left side moves out concurrently as the right core moves in, thereby resulting in both inward and outward inductance changes. The geometry of these coils, is discussed in subsequent sections.

The force, F_{core}, applied on the core is given by:

$$F_{core} = ma = m\left(\frac{\delta}{\delta t}\frac{\delta x}{\delta t}\right) = m\left(\frac{\delta^2 x}{\delta t^2}\right) = PA \qquad (1)$$

In the case of differential pressure, the above equation becomes

$$\left(\frac{(P - P_{wind})A}{m}\right) = \frac{\delta^2 x}{\delta t^2} = a \tag{2}$$

The inductance of the coil when the core is moving out by displacement 'x' as a result of force as seen on the right side of Figure 1, is given by:

$$L_{IN} = \frac{\mu_o N^2 A}{l}\left(\frac{x}{l} + \mu_r\left(1 - \frac{x}{l}\right)\right) \tag{3}$$

3.1.Dynamic Range Of Core Geometry As A Result of inward Position Displacement

When the core goes out from the coil geometry, simultaneously the second core on the other side moves in, the inductive change is hence as derived in Appendix I to be given as a function of acceleration is as shown:

$$L_{IN} = \frac{\mu_o N^2 A}{2l^2}\left(\mu_r 2l + at^2(1 - \mu_r)\right) \tag{4}$$

While as a function of speed with which the core goes outside the coils is derived as:

$$L_{IN} = \frac{\mu_o N^2 A}{2l^2}\left[\mu_r 2l + vt(1 - \mu_r)\right] \tag{5}$$

3.1.1 The Position of Core As A Function of Differential Pressure on The Inductance

The cores moving in and out of the coils geometry has a weight define as:

$$W = mg = (P - P_{wind})A$$

But the acceleration due to gravity or the magnetic field strength g and details of equation 8 are found in appendix I.

$$\frac{(P - P_{wind})At^2}{2m} = x \tag{6}$$

Equation 6 gives the relation between the position displacement and the differential pressure acting on the core as a result of oscillation in the seesaw. The inductance as a result of the position of the core as a function of the differential pressure with respect to the outward inductance of the core is given in (7).

$$L_{IN} = \frac{\mu_o N^2 A^2 t^2}{2ml^2}\left(2ml\mu_r + (1 - \mu_r)(P - P_{wind})\right) \tag{7}$$

3.1.2. The Position of Core Outward Motion as a Function of Differential Pressure To Frequency

From the original frequency of equation derived in previous work, its frequency was obtained as a function of change in inductance and the resistance of the circuit as:

$$f = \frac{1.58R}{L} = \frac{3.16Rml^2}{\mu_o N^2 A^2 t^2\left(2ml\mu_r + (1 - \mu_r)(P - P_{wind})\right)} \tag{8}$$

3.1.3. The Position Of Core Outward Motion As A Function Of Speed To Frequency Output

From appendix II, the frequency as a function speed is obtained as shown in (9)

$$f = \frac{3.16 R l^2}{\mu_o N^2 A t \left(\mu_r 2l + v(1 - \mu_r) \right)}$$ **(9)**

3.1.4. The Position of Core Inward Motion as A Function Of Acceleration To Frequency Output

The acceleration of the core into the coil geometry was given as:

$$L = \frac{\mu_o N^2 A}{2l^2} \left(\mu_r 2l + at^2(1 - \mu_r) \right)$$

If the frequency output was obtained from the timer, the frequency as a function of acceleration is;
Details of derivation is shown in appendix

$$f = \frac{3.16 R l^2}{\mu_o N^2 A t^2 \left(\mu_r 2l + a(1 - \mu_r) \right)}$$ **(9)**

3.1.5. Position of Core inward Motion as a Function of Displacement to Frequency Output

Substituting the inductance into frequency produces; details of derivations are shown in appendix II.

$$f = \frac{1.58 R l^2}{\mu_o N^2 A \left(\mu_r l + x(1 - \mu_r) \right)}$$ (10)

3.2 Dynamic Range of Core Geometry as a Result of Outward Position Displacement from a Seesaw Oscillation

When the core goes out from the coil geometry simultaneously from the other side of the seesaw bar orientation, the inductive change of the outward movement of the core is thus given by:

$$L_{OUT} = \frac{\mu_o N^2 A}{l} \left(\mu_r \frac{x}{l} + \frac{l - x}{l} \right) = \frac{\mu_o N^2 A}{l} \left(1 + \frac{x}{l}(\mu_r - 1) \right)$$

3.2.1. Inductance Change as a Function of Acceleration From The Inward Movement Of The Core In The Seesaw Oscillation

The equation may further be related to acceleration as given in substituting equation 2 into the outward inductance we have equation 11 while the details are shown in appendix III.

$$L_{OUT} = \frac{\mu_o N^2 A}{2l^2} \left(2l + at^2(\mu_r - 1) \right)$$ (11)

3.2.2. Inductance Change as a Function of the Outward Speed of The Core

Substituting v=at into the outward inductance and differential pressure equation, we have;

$$L_{OUT} = \frac{\mu_o N^2 A^2 t^2}{2ml^2} \left(2ml + (P - P_{wind})(\mu_r - 1) \right)$$ **(12)**

The Inductance change with net Force applied;

$$L_{OUT} = \frac{\mu_o N^2 A t^2}{2l^2}\left(2l + F(\mu_r - 1)\right) \tag{13}$$

3.2.3. The Position of Outward Core as a Function of Pressure to Frequency

Substituting the differential pressure and inductance into the frequency equation, we have;

$$f = \frac{3.16 R m l^2}{\mu_o N^2 A^2 t^2 \left(2ml + (P - P_{wind})(\mu_r - 1)\right)} \tag{14}$$

Details of the derivations are shown in appendix III

3.2.4. Position of Outward Core as a Function of Force to Frequency

From our earlier derived and published equation of frequency, we had;

$$f = \frac{1.58R}{L} = \frac{3.16 m R l^2}{\mu_o N^2 A t^2 \left(2l + F(\mu_r - 1)\right)} \tag{15}$$

3.2.5. The Position of the Outward Core as a Function of Acceleration to Frequency

Substituting acceleration equation into frequency equation, we have and the details are shown in appendix III;

$$f = \frac{3.16 R l^2}{\mu_o N^2 A \left(2l + a t^2 (\mu_r - 1)\right)} \tag{16}$$

3.2.6. The Position of the Outward Core as a Function of Displacement to Frequency

Substituting the outward inductance equation into frequency equation, we have;

$$f = \frac{1.58R}{\frac{\mu_o N^2 A}{l}\left(1 + \frac{x}{l}(\mu_r - 1)\right)} = \frac{1.58 R l}{\mu_o N^2 A \left(1 + \frac{x}{l}(\mu_r - 1)\right)} \tag{17}$$

4. ANALYTICAL RESULTS AND DISCUSSIONS

A simulation of the designed mathematical model and its necessary derivations for inductive behavior when differential pressure is applied from both arms of the convulsion bar oscillating according the difference in the applied pressure or force result to inductance, frequency, kinematics when motion parameters are varied. The results are segmented in subsection 4.1-4.3.

4.1. Inductive Change From Differentially Applied Pressure With Acceleration, Speed And Displacement

When the magnetic core from the right arm of the convulsion bar goes into the coil geometry as a result of differential pressure brought about by the wind/air ambient, and acting force on the seesaw over an area, then the acceleration of the movement of the core is obtained which is proportional to the inductance parameter. From Fig. 3 (a), the inductance increases as the core accelerate at higher rate. From the left arm of the bar, the inductance reduces the core decelerate from the coil topological geometry. This same as in the case of speed from Fig. 3 (b). Since speed increases as an object accelerate faster, hence, the graph

shows the same result. From the right arm, when the core goes into the coils, the inductive variation increases with increase in speed and its lowered from the left side as the speed decreases. Also, from Fig. 3 (c), the inductance increases from the right arm as more length of the coil is displaced and decreases as the core leaves the coil geometry. Fig. 3 (d) shows a linear variation in the inductance against the displacement. Fig. 3 (e) shows the inductive from both arms with various density of the air force. The inductance in this case increases as the core goes in and decreases as the core goes out.
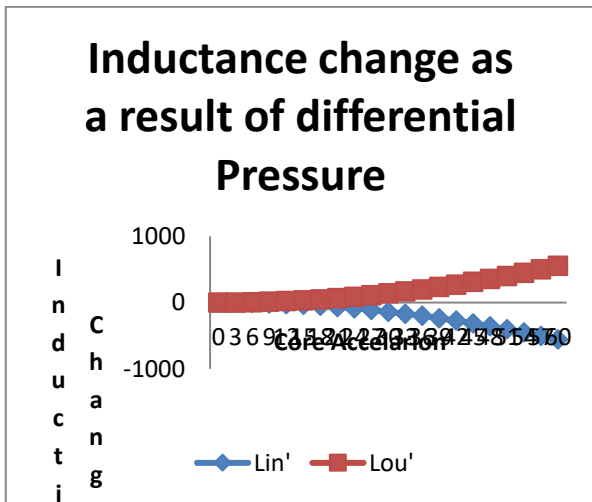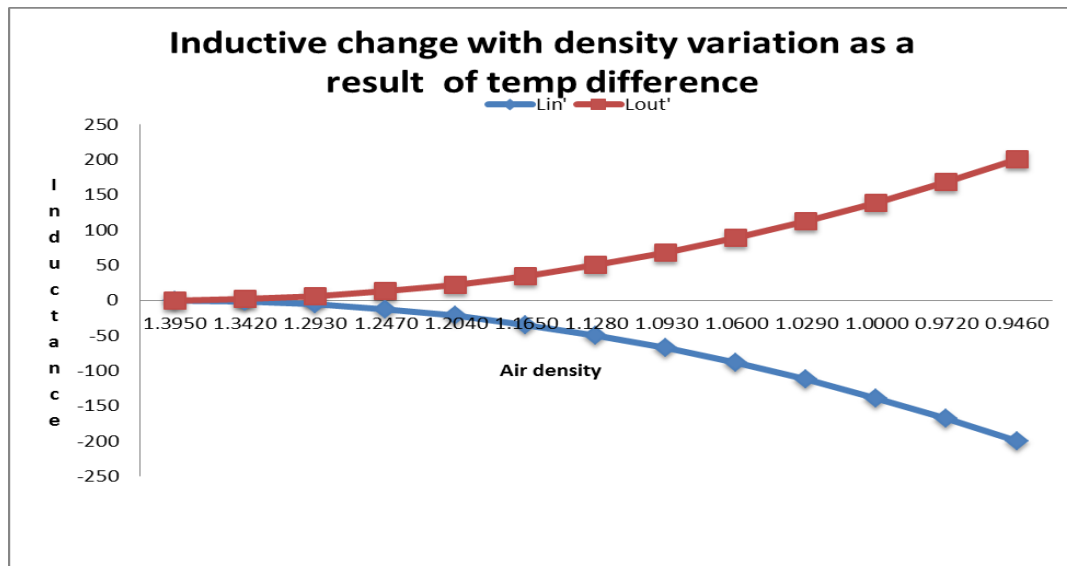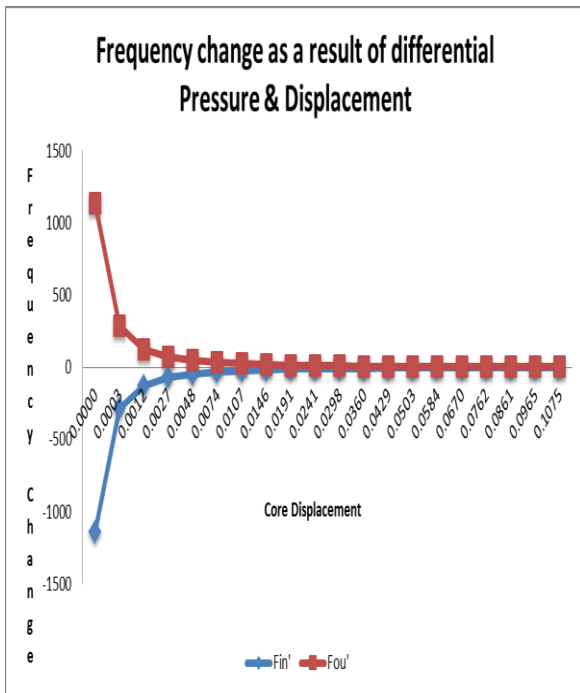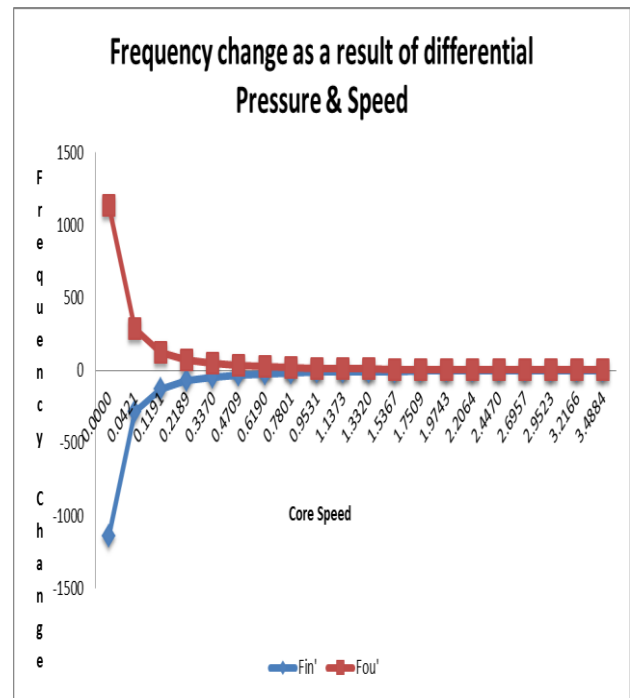

(a)
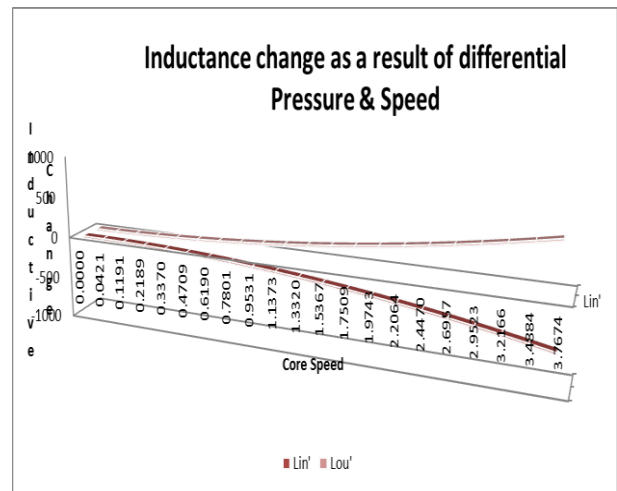
(b)
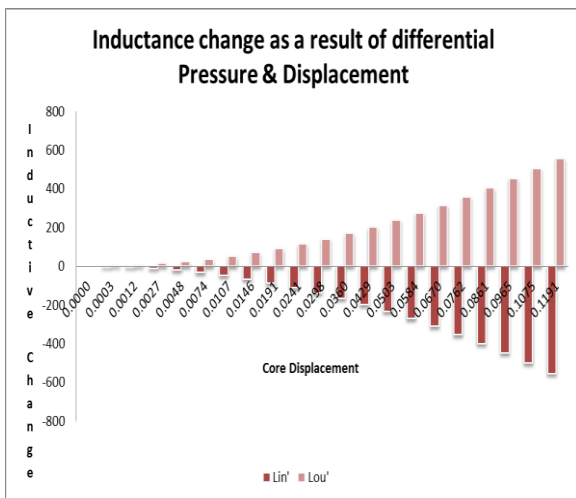
(c)
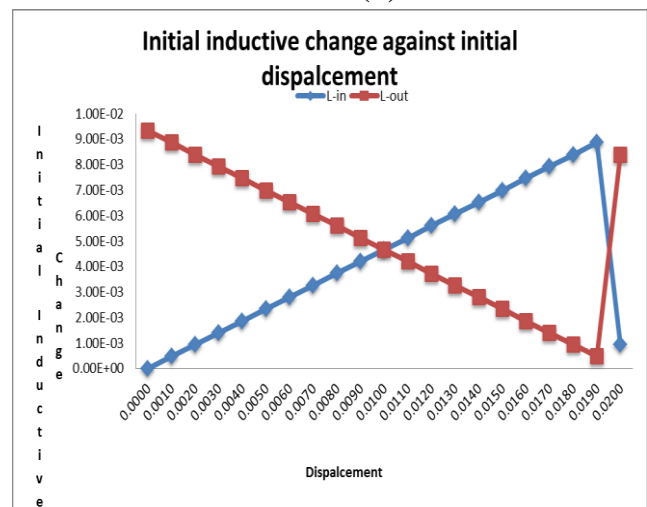
(d)

(e)

Fig. 3(a): Shows inductive change as a function of differential pressure with core acceleration, (b): Shows inductive change as a function of differential pressure with core speed, (c): Shows inductive change as a function of differential pressure with core displacement and (d): Shows the initial inductive as a function of inductance only with displacement, (e): Shows inductive change with density of air variation as a result of temperature difference.

4.2. Frequency Change From Differentially Applied Pressure With Acceleration, Speed And Displacement

From Fig. 1 as seen from the core insertion technique brought about by the seesaw oscillation mechanism, caused by differential pressure, the sensed parameter is fed into a processor, which in this case, is a timer circuit for characteristic linearization of second and third derivative of the model. The processor characterizes these sensed parameter and converts it into a useful electrical signal based sequence of instruction. While attuning with the sensed parameters of speed, acceleration, displacement, a signal of interest such as frequency is obtained from the output pin 3 of the timer. These frequencies are affected by the great influence of the differential causing the core motion in vertical orientation. From Fig 4 (a-d), the frequency of the output signal increases as the core goes into the geometrical coil space. The frequency decreases geometrically as the core goes out of the coil orthogonal orientation. The result of frequency with displacement, speed, acceleration are similar because as the core accelerate more, then the speed increases and hence, more length is displacement ultimately.
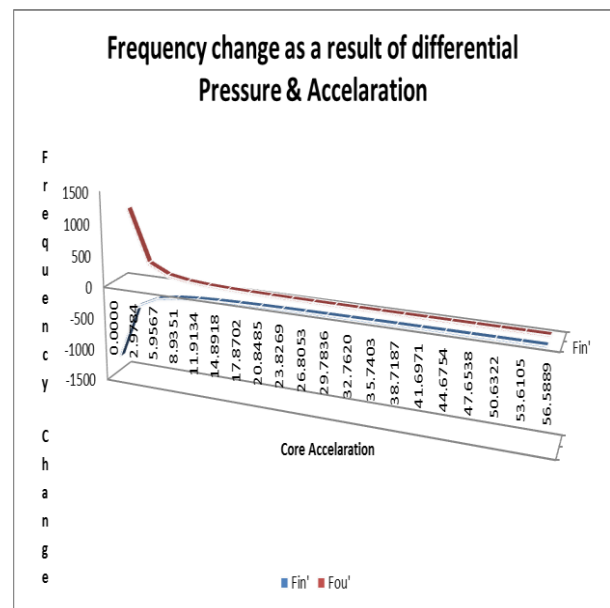
(a)

(b)
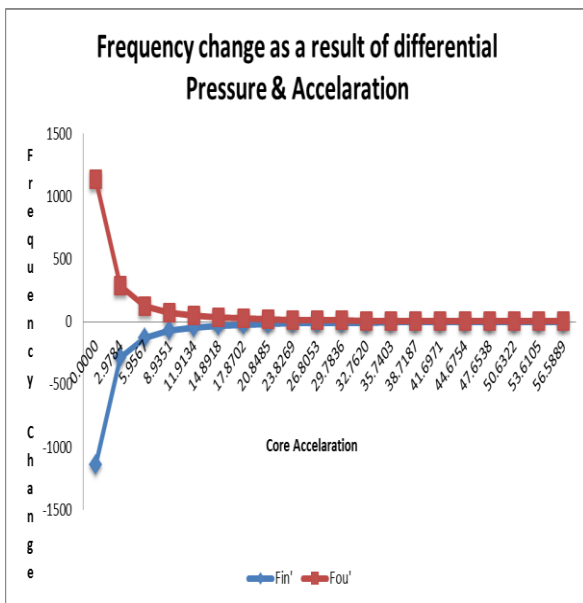
(c)

(d)

Fig. 4(a): Shows frequency change as a function of differential pressure with core displacement, (b): Shows frequency change as a function of differential pressure with core speed, (c): Shows frequency change as a function of differential pressure with core acceleration and (d): Shows a 3D frequency change as a function of differential pressure with core acceleration.

4.3.Kinematics from Differentially Applied Air Density, Pressure difference and Time.
Fig 5 (a-c) shows the acceleration, speed and displacement of the core against air density causing pressure, pressure difference and time. From the result in Fig.5a, it shows that the acceleration was uniform. This means that as the air density due to temperature change increases, the magnetic core accelerate faster.
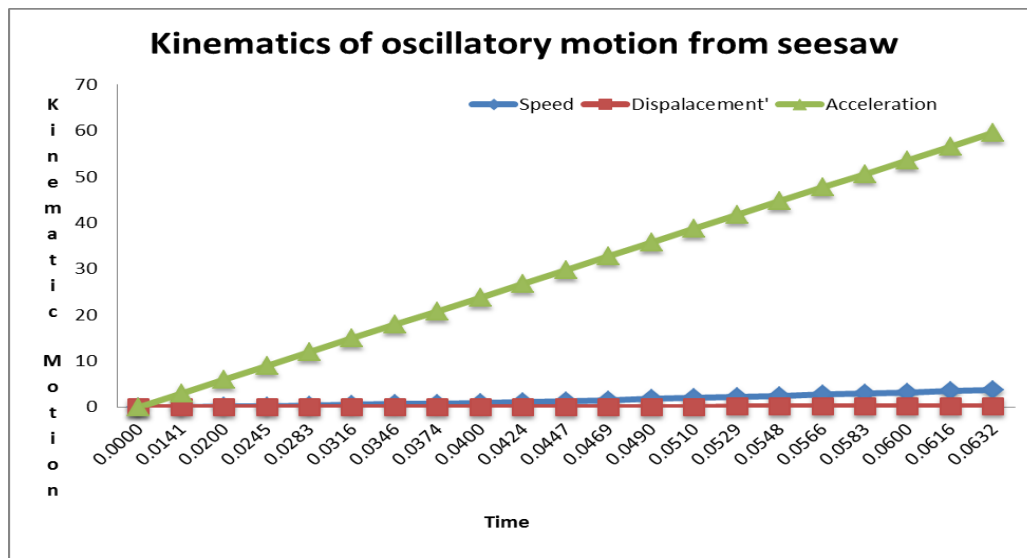
However, the speed and displacement have values obtained which close to the air density causing the pressure difference, and hence the motion. Also, Fig. 5(a) and (b) have similar result. This shows that the density is a major pressure causing parameter especially atmospheric pressure.
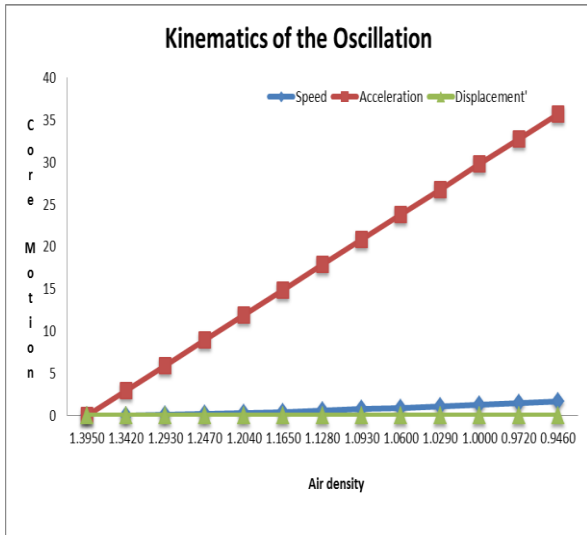

(a)
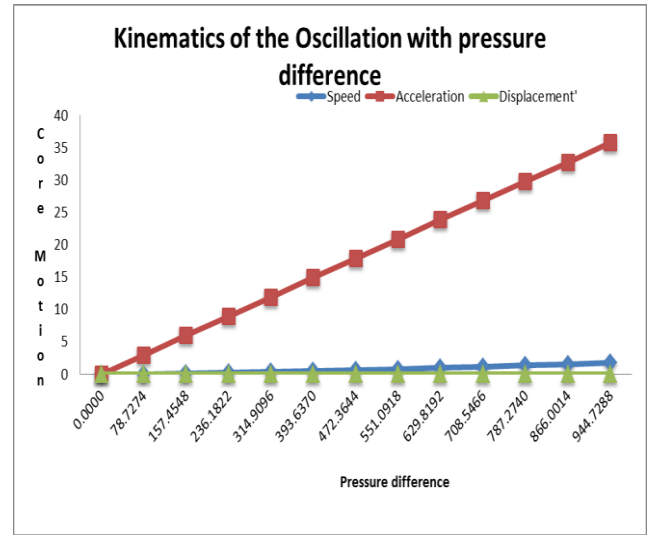
(b)

(c)

Fig. 5 (a) kinematic motion of the seesaw against air density, (b) Kinematic motion of the seesaw against pressure difference, (c) Kinematic motion of the seesaw against time.

## 4.4 Frequency as A Function of The Resistor and Time Period

From the sensing mechanism, an output frequency has been determined as an improvement to the existing work in this area. This output frequency from sensor have been obtained in equation 16 and 17. These two frequencies from the sensor and processor are then compared, analyzed, being combined and sent to the display such as register, counter for storage and other usage. From Figure 6 (a)-(b), the frequency from the sensor is a linearized one which is a much improvement to the one in literature [1-19]. The frequency from the timer is galloping as it's just the reciprocal of the time period when considered with resistor and

inductor. From Figure 6 (a), the values of the resistor have been varied. This shows that the value of the frequency increases and the resistive value increases from both sensor and timer. However, the timer as it where, gives a sinusoidal effect of the frequency.

Again, making the value of the resistor constant and varying the inductive value result in Figure 4.14(b). Here, the frequency decreases as the inductive value increases while resistor becomes constant. Hence, if the resistor is fixed while varying the inductive value, the sensor's position measurement will be such that the increase inductive change negates the resulting output frequency from all combinations.
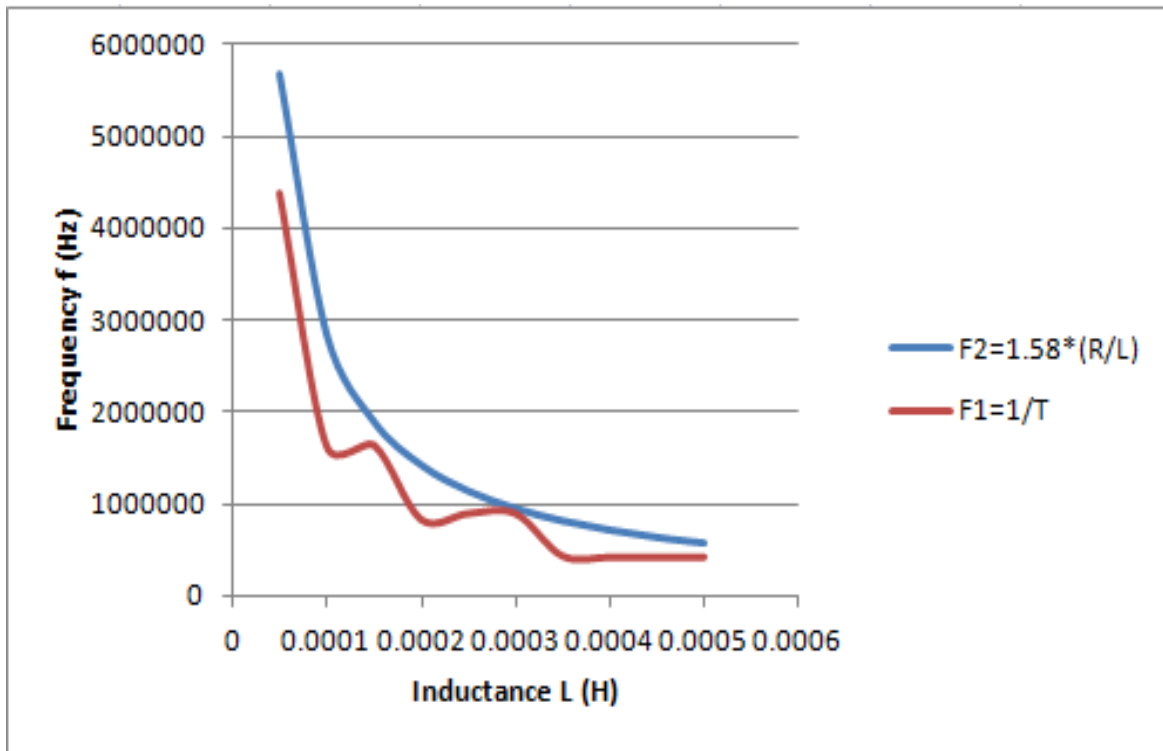
(a)
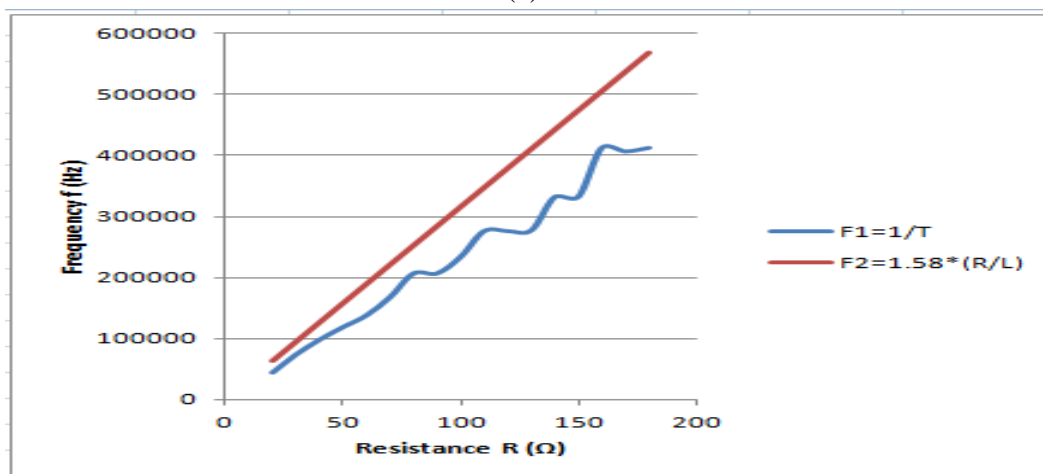
(b)

Figure 6: (a) Frequency with varying inductors and resistors from the timer and sensor. (b) Frequency with varying inductors and fixed resistor from the timer and sensor

5. CONCLUSION

A mathematical characterization modeling approach of an inductive oscillating sensor using core displacement, in magnetic coil orientation, hence characterizing the speed, acceleration and frequency of the proposed differential inductive coupling. This model uses double coil arrangement with magnetic core made of iron suspended in a seesaw. This is made to oscillate freely thereby producing the proposed characterization. This is produces a pressure sensor, force sensor, vibrator sensor, propelled by wind force and vibration which are used for the acquisition of impulsive electrical signal from a harsh environmental location and/or a machine vibration which can slowly set the seesaw into oscillation and therefore producing helpful speed, acceleration and frequency generating models. Using an inductive coil sensing technique in a differential manner, a physical parameter such as speed, acceleration and displacement are translated into a signal with proportionate output frequency change. The results shown can be used for characterizing the materials and hence sensor with high sensitivity, linearity and responsiveness in harsh environmental condition is obtained. The result obtained verifies the derivations and the simulation in literature [2]-[4]. The error is brought to minima value of 0.01% of FSO.

REFERENCES

1. Mohamed A.S and Soliman A.M., (2017) " A novel study of using Oil Refinery Plants waste gases for Thermal Desalination and Electric Power Generation: Energy, exergy and Cost Evaluation" "Elsevier Journal on Applied Energy. 195 (2017) 453-477.

2. Mohamed A.S, Adel E.S and Soliman A.M., (2017) "A New Modeling Technique Based on Performance Data for Photovoltaic Modules and Horizontal Axis Wind Turbines" "A research Article on Wind Engineering and SAGE. (2017) 1-21.

3. European Commission, "BREF on the surface treatment of metals and plastics," BAT (Best Available Techniques) Reference Document (BREF), Aug. 2006.

4. *Ezzat, G.B. and H.M. Marvin Cheng, AUGUST 2011. "High-Sensitivity Inductive Pressure Sensor," IEEE Transactions on Instrumentation And Measurement, 60(8).*

5. Khan S., A. Deji, A.H.M Zahirul, J. Chebil, M.M Shobani, A.M Noreha. (Setember 2012)"Design of a Differential Sensor Circuit for Biomedical Implant Applications". *Australia. Journal of Basic and Applied. Sciences., 6(9): 1-9.* 10.1002/9781118329481.ch1.

6. Jeevandoss, C.R., M. Kumaravel and V.K. Jagadeesh, 2011. "A Novel Measurement Method to Determine the *C–V* Characteristic of a Solar Photovoltaic Cell". *IEEE Trans. Instrum. Meas.*, 60 (5): 1761-1767.

7. Shuenn-Yuh, L., C. Cheng and M.C. Liang, 2011 "A Low-Power Bidirectional Telemetry Device with a Near-Field Charging Feature for a Cardiac Microstimulator" *IEEE Transactions on Biomedical Circuits and Systems,* 5(4): 357-367.

8. *John, W.J., A.S. Raymond, 2008. "Physics for scientists and engineers with modern physics" 7th edition. Department of Physics and Astronomy, Georgia State University "Magnetic Properties of Ferromagnetic Materials table" 2001- Online at http://hyperphysics.phy-astr.gsu.edu/HBASE/Tables/magprop.html . Texas Instruments, "LM555 Data sheet" 2003.*

9. Slawomir, T., (2007) "Induction coil sensors—a review" Institute Of Physics Publishing Measurement Science And Technology, Institute of Electrical Theory & Measurement, ul Koszykowa 75, 00-661 Warsaw, Poland. Meas. Sci. Technol. 18 R31–R46.

10. Mohammed, S. S, A. B. George, L. Vanajakshi, and J. Venkatraman, May 2012. "A Magnetically Coupled Inductive Loop Sensing System for Less-lane Disciplined Traffic," in *Proc. IEEE I2MTC*, Graz, Austria, pp. 827–834.

11. Mohammed, S. S, A. B. George, L. Vanajakshi, and J. Venkatraman, MAY 2012. "A Multiple Inductive Loop Vehicle Detection System for Heterogeneous and Lane-Less Traffic," IEEE Transactions on Instrumentation and Measurement, Vol. 61, No. 5, 1353-1361.

12. Ripka, P., (2001). Induction sensors Magnetic Sensors and Magnetometers (Boston, MA: Artech House) pp 47–74 chapter 2

13. Mohan, N. M., Shet A. R., Kedarnath S., and Kumar V. J., (2008). "Digital Converter for Differential Capacitive Sensors," IEEE TRANSACTIONS on Instrumentation and Measurement, Vol. 57, No. 11, pp.: 2576-2581.

14. Mohan, N. M., George A. B., and Kumar V. J., (2009). *"Analysis of a Sigma–Delta Resistance-to-Digital Converter for Differential Resistive Sensors,"* IEEE Transactions on Instrumentation and Measurement, Vol. 58, NO. 5, 1617-1622

15. Ravindra W., (2006). 'Inductive Fiber-Meshed Strain and Displacement Transducers for Respiratory Measuring Systems and Motion Capturing Systems' IEEE Sensors Journal, Vol. 6, No. 3.

16. Udaya K. M., and Duleepa J. T., (2011), "A Bidirectional Inductive Power Interface for Electric Vehicles in V2G Systems," IEEE TRANSACTIONS ON INDUSTRIAL ELECTRONICS, VOL. 58, NO. 10, pp. 4789-4796.

17. Zhang, F., Holleman J., and Otis B.P., (2012). "Design of Ultra-Low Power Bio potential Amplifiers for Bio-signal Acquisition Applications," IEEE Transactions On Biomedical Circuits And Systems, Vol. 6, NO. 4.

18. Deji A., Sheroz K, Musse M.A, Jalel C. (August 2014). Analysis and evaluation of differential inductive transducers for transforming physical parameters into usable output frequency signal August 2014 International Journal of the Physical Sciences 9(15):339-349 DOI:10.5897/IJPS12.655

APPENDIX I

$$L_{IN} = \frac{\mu_o N^2 A}{l}\left(\frac{x}{l} + \mu_r\left(1 - \frac{x}{l}\right)\right)$$

$$L_{IN} = \frac{\mu_o N^2 A}{l}\left(\frac{at^2}{2l} + \mu_r\left(1 - \frac{at^2}{2l}\right)\right)$$

$$L_{IN} = \frac{\mu_o N^2 A}{l}\left(\frac{at^2}{2l} + \frac{\mu_r}{1} - \frac{\mu_r at^2}{2l}\right)$$

Simplifying the above equation, we have;

$$L_{IN} = \frac{\mu_o N^2 A}{l}\left(\frac{at^2 + \mu_r 2l - \mu_r at^2}{2l}\right)$$

$$g = \frac{2x}{t^2}$$

Assuming that $a = g$ and making all necessary substitutions, we have;

$$(P - P_{wind})A = \frac{2mx}{t^2}$$

Cross multiplying

$$(P - P_{wind})At^2 = 2mx$$

Dividing both sides by $2m$, we have;

Substituting equation 8 into 3, we have:

$$L_{IN} = \frac{\mu_o N^2 A}{l}\left(\frac{(P - P_{wind})At^2}{\frac{2m}{l}} + \mu_r\left(1 - \left[\frac{P - P_{wind}}{\frac{2m}{l}}\right]At^2\right)\right)$$

$$L_{IN} = \frac{\mu_o N^2 A}{l}\left(\frac{P - P_{wind}}{2ml}\right)At^2 + \frac{\mu_r}{1}\left(\frac{1 - (P - P_{wind})At^2}{2ml}\right) \qquad L_{IN} =$$

$$\frac{\mu_o N^2 A}{l}\left(\frac{(P - P_{wind})At^2 + 2ml\mu_r\left(1 - (P - P_{wind})At^2\right)}{2ml}\right)$$

APPENDIX II

Substituting equation 9 into frequency equation, we have;

$$f = \frac{1.58R}{\frac{\mu_o N^2 A^2 t^2}{2ml^2}\left(2ml\mu_r + (1 - \mu_r)(P - P_{wind})\right)}$$

$$f = \frac{1.58R * 2ml^2}{\mu_o N^2 A^2 t^2\left(2ml\mu_r + (1 - \mu_r)(P - P_{wind})\right)}$$

$$L = \frac{\mu_o N^2 A}{2l^2}t\left(\mu_r 2l + v(1 - \mu_r)\right)$$

$$f = \frac{1.58R}{L}$$

$$f = \frac{1.58R}{\frac{\mu_o N^2 A}{2l^2}\left(\mu_r 2l + v(1 - \mu_r)t\right)}$$

$$f = \frac{1.58R}{\frac{\mu_o N^2 A}{2l^2}\left(\mu_r 2l + at^2(1 - \mu_r)\right)}$$

$$f = \frac{1.58R * 2l^2}{\mu_o N^2 A\left(\mu_r 2l + at^2(1 - \mu_r)\right)}$$

$$f = \frac{1.58Rl}{\mu_o N^2 A\left(\frac{x}{l} + \mu_r\left(1 - \frac{x}{l}\right)\right)}$$

Rearranging the above equation, give rise to equation 13;

APPENDIX III

$$L_{OUT} = \frac{\mu_o N^2 A}{l}\left(\mu_r \frac{at^2}{2l} + \frac{l - at^2}{2l}\right) = \frac{\mu_o N^2 A}{l}\left(1 + \frac{at^2}{2l}(\mu_r - 1)\right) \qquad L_{OUT} = \frac{\mu_o N^2 A}{l}\left(\frac{2l + at^2}{2l}(\mu_r - 1)\right)$$

$$L_{OUT} = \frac{\mu_o N^2 A}{2l^2}\left(2l + vt(\mu_r - 1)\right)$$

From 14,

$$L_{OUT} = \frac{\mu_o N^2 A}{l}\left(1 + \frac{(P - P_{wind})At^2}{2ml}(\mu_r - 1)\right)$$

$$L_{OUT} = \frac{\mu_o N^2 A}{l}\left(\frac{2ml + (P - P_{wind})At^2}{2ml}(\mu_r - 1)\right) \quad \text{From equation 16,}$$

$$f = \frac{1.58R}{\frac{\mu_o N^2 A^2 t^2}{2ml^2}\left(2ml + (P - P_{wind})(\mu_r - 1)\right)}$$

$$f = \frac{1.58R \times 2ml^2}{\mu_o N^2 A^2 t^2 \left(2ml + \left(P - P_{wind}\right)\left(\mu_r - 1\right)\right)}$$

From equation 18,

$$f = \frac{1.58R}{\frac{\mu_o N^2 A}{2l^2}\left(2l + at^2\left(\mu_r - 1\right)\right)}$$

$$f = \frac{1.58R \times 2l^2}{\mu_o N^2 A\left(2l + at^2\left(\mu_r - 1\right)\right)}$$

$$L_{IN} = \frac{\mu_o N^2 A}{2l^2}\left(\mu_r 2l + at^2 - \mu_r at^2\right)$$